JOC The Journal of Organic Chemistry

Article

pubs.acs.org/joc

Phenanthrylene-butadiynylene and Phenanthrylene-thienylene Macrocycles: Synthesis, Structure, and Properties

Bhimrao Vaijnath Phulwale,[†,‡] Sushil Kumar Mishra,[‡] Marek Nečas,[†,‡] and Ctibor Mazal*[,†,‡]

[†]Department of Chemistry, Faculty of Science, Masaryk University, Kotlářská 2, 611 37 Brno, Czech Republic

[‡]CEITEC - Central European Institute of Technology, Masaryk University, Kamenice 5, 625 00 Brno-Bohunice, Czech Republic

Supporting Information

ABSTRACT: A series of macrocycles consisting of 9,10-substituted phenanthrenes connected by butadiynylene linkers in positions 3 and 6 has been described as well as their transformation into the corresponding phenanthrylene-thienylene macrocycles. Structure and properties of the macrocycles, such as self-association in solution and optical and electrochemical properties, were studied and reported in a comparative manner with respect to the effects of the different sizes and shapes of the macrocycles and the character and length of their side chains.

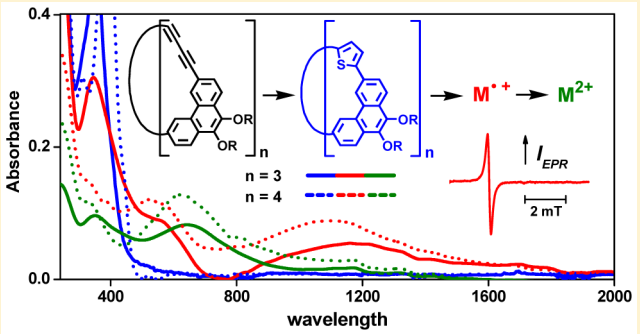

INTRODUCTION

Over the years, several approaches to construct $\pi-\pi$ conjugated shape-persistent macrocycles have been introduced.[1] The arylene-ethynylene cores proved to be very attractive since arenes offer a sufficient geometrical variability of the building blocks, and alkyne chemistry provides numerous methods to link them together.[2] Moreover, the alkyne linkage is linear and assures full conjugation. So far, phenanthrene derivatives have seldom been used as the arylene building blocks in the syntheses of macrocycles. Among other geometrical features, phenanthrene offers a 60° angle formed between its positions 3 and 6 suitable for construction of equilateral triangular macrocycles and leaves the easy transformable positions 9 and 10 for the connection of various flexible substituents that can balance expected sturdiness of macrocycle backbone and increase its solubility and processability. These phenanthrene features were used in the preparation of self-assembled supramolecular organoplatinum macrocycles,[3] macrocyclic boronates,[4] and Schiff bases.[5] Recently, the phenanthrene building blocks were used in combination with acetylene linkers[6] and also with a bulky σ-bonded diyne linker that hindered conjugation as well as $\pi-\pi$ stacking of the molecules.[7] Another arylene building block that has been attracting increasing attention for the past several years is thiophene, widely used in syntheses of fully π-conjugated macrocycles[8] with high potential in materials science applications, such as organic field effect transistors,[9] organic light emitting diodes, organic solar cells,[10] molecular switching devices, liquid crystalline materials[11] or nonlinear optics.[12] Incorporation of electron rich thiophenes into cores of fully conjugated shape persistent macrocycles markedly changes their structural and electronic properties, and transformation of the diyne linkages into the thienylene ones in various arylene-butadiynylene macrocycles thus offers a feasible way to do it.

RESULTS AND DISCUSSION

We have synthesized a series of macrocycles as formal cyclic oligomers of 9,10-dialkoxy-3,6-phenanthrylenediacetylenes and obtained their thiophene analogues by transformation of the butadiynylene linkers into the 2,5-thienylene ones. That enabled us to study both series of the macrocycles in a comparative manner in order to understand some structure–property relationships, such as self-assembly, optical properties, and electrochemical properties with respect to their different composition, size, and geometry.

The butadiynylene macrocycles **1** and **2** have been synthesized according to Scheme 1 from their diyne precursors **3** by palladium catalyzed oxidative coupling. A very similar procedure was published by He et al.[6] for the preparation of **1b** in the course of our work. In our case, however, the precursors **3** and subsequently the target products varied in 9,10-alkoxysubstituents of their phenanthrylene units. Besides the hexyloxy chains used in the mentioned study, methoxy, butoxy, decyloxy, and more polar glycol ether chains were used as the peripheral substituents. They were introduced into the very starting 3,6-dibromophenanthroquinone using various proven procedures[5,7,13] of its 9,10-derivatization to **4** which then provided protected diynes **5** by the Sonogashira cross-coupling reaction. An oligocyclization of the deprotected diynes **3** afforded satisfactory yields (30–42%) of the main products, the triangular macrocycles **1a–e**. Cyclic tetramers **2** were also

Received: April 12, 2016
Published: July 11, 2016

DOI: 10.1021/acs.joc.6b00814
J. Org. Chem. 2016, 81, 6244–6252

Scheme 1. Synthesis of Phenanthrylene-butadiynylene Macrocycles

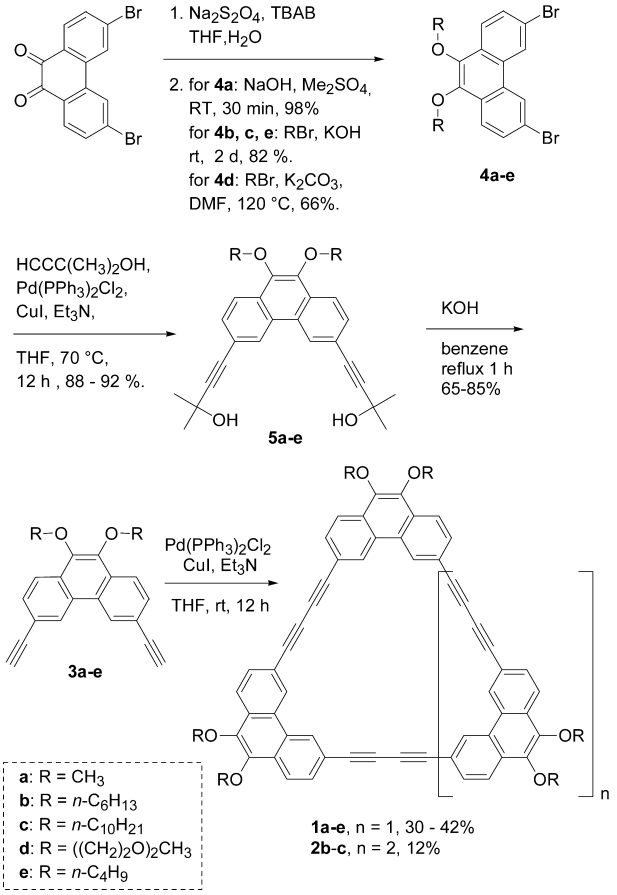

detected in the crude reaction mixtures, but only **2b** and **2c** were isolated in about 12% yields for a difficult separation of the other tetramers **2** from higher oligomers and a polymer. Interestingly, the cyclic dimer that was formed in about 10% in the published procedure[6] for **1b** was not observed in our case. The higher cyclic oligomers were detected instead by NMR and MALDI-MS;[14] however, none of them was isolated except for the tetramers mentioned.

Butadiynylene bridges in the macrocycles **1** can be easily transformed into the 2,5-thienylene ones by the reaction with sodium sulfide in ethylene glycol methyl ether (EGME) and toluene (Scheme 2). The method that appeared in early 1960s[15] was probably first used for the transformation of an endocyclic butadiyne unit by Acheson and Lee[16] and recently gained in popularity for the introduction of 2,5-thienylene into various macrocycles.[17] The reaction ran well with all our triangular macrocycles **1a−d** as well as with the tetramer **2c** that was isolated in a satisfactory amount for that purpose. While **1a−d** gave stable products **6a−d**, the tetramer **2c** afforded **7c**, apparently more sensitive to air oxidation, which has to be considered in its handling.

The oxidation of some thiophene containing macrocycles has already been described,[18,19] but the ease with which it occurred in the case of **7c** was surprising in comparison with that of the macrocycles **6**. A slow oxidation of NMR samples of **7c** dissolved in $CDCl_3$ by air was noticed, so a sample was purposely oxidized by addition of 2,3-dichloro-5,6-dicyano-1,4-benzoquinone (DDQ). The solution turned black immediately, and signals of aromatic protons disappeared from the ^1H NMR

Scheme 2. Synthesis of Thienylene-phenanthrylene Macrocycles

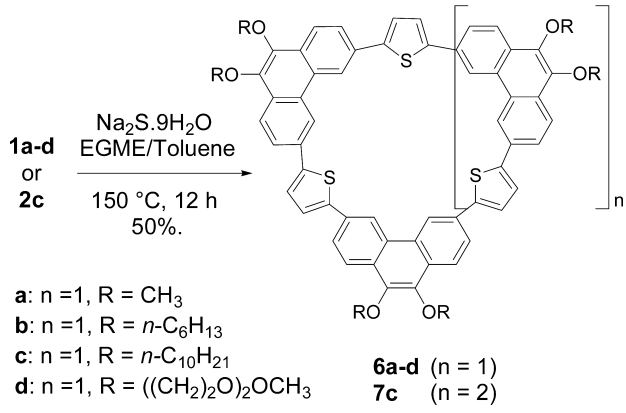

spectrum due to the paramagnetism of the radical cation formed (Figure 1). Addition of magnesium turning or washing

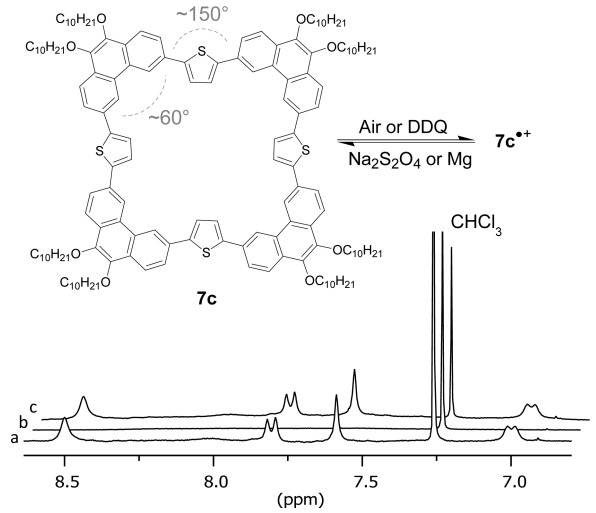

Figure 1. (a) Details of the ^1H NMR spectra of **7c** in $CDCl_3$; (b) that after oxidation with DDQ; (c) after washing the sample with aqueous $Na_2S_2O_4$.

with aqueous $Na_2S_2O_4$ regenerated the original yellowish color of the sample, and also, the NMR signals appeared again. That indicated a reversible oxidation of **7c** to a radical cation.[19,20] A noticeable decrease of the residual $CHCl_3$ concentration in the NMR sample in the course of the redox reaction was probably due to its involvement in the radical processes and high kinetic isotope effect of H/D abstraction.[21] Further evidence of the cation radical formation given by spectroelectrochemical measurements is mentioned later. It has to be noted that the NMR samples of **7c** in C_6D_6 were stable.

The ease of **7c** oxidation in comparison with that of **6a−d** can be explained partly by differences in geometry of the macrocycles partly by the extent of their conjugated π-systems. Transformation of linear butadiynylene linkers of planar triangular macrocycles **1** into the angled 2,5-thienylenes in **6** deteriorates the molecular planarity and so the π-system delocalization. However, whereas the macrocycles **2** can hardly adopt a planar conformation, the alternate concave and convex orientation of phenanthrylene and thienylene building blocks in **7c** enables both planarity (cf. Figure 1) and better delocalization of its larger electron rich π-system. This

DOI: 10.1021/acs.joc.6b00814
J. Org. Chem. 2016, 81, 6244−6252

facilitates the oxidation. The mutual orientation of phenanthrylene and thienylene building blocks was confirmed by ^{1}H−^{1}H ROESY NMR measurement (Figure 2). In **7c**, an

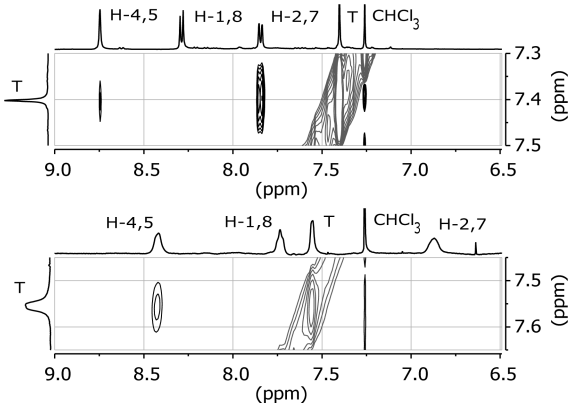

Figure 2. Details of ^{1}H−^{1}H ROESY NMR spectra of **6c** (upper panel) and **7c** (bottom panel) which show cross-peaks of the thiophene protons (T) and the corresponding phenanthrene protons (H-2,7 and H-4,5) suggesting the mutual orientation of the rings in the macrocycles.

interaction was found between the thiophene protons and inner protons of the phenanthrene rings (H-4 and H-5). A similar ROESY experiment with **6c** shows that the thiophene protons interact with inner as well as with outer phenanthrene protons (H-4,5 and H-2,7). The thiophene rings thus adopt both concave and convex orientations in the macrocycle. Relative intensities of the corresponding cross-peaks suggest that the concave orientation prevails.

These results are in good agreement with a density functional theory (B3LYP/6-31G(d, p)) structure optimization that shows nearly planar **7a** with convex-oriented thiophene rings twisted slightly out of plane, releasing thus the repulsion with phenanthrene hydrogens (Figure 3, bottom panel). The DFT minimized structure of **6a** shows one convex- and two concave-oriented thiophene rings in a saddle-like structure (Figure 3, upper panel), but very likely, the macrocycle is conformationally flexible, and the "all-concave" conformer is also present as obvious from relative integral intensities of the corresponding cross-peaks in the ROESY spectrum. Similar calculations confirmed the planarity of **1a**, whereas a wing-shaped geometry was found for the "tetramer" **2a** with the wing angle approximately 74°.

A self-association of **1b** due to $\pi-\pi$ stacking has been described,[6] and the corresponding association constant was calculated from a shift of ^{1}H NMR signals with concentration using a simple dimer model.[22] Being aware of the shortcomings of the model, we used it in order to get a comparison with the previous data and calculated K_{ass} for all macrocycles **1a−e** and also for **6a−d** and **7c** where a shift of the signals was also observed (Table 1). The results obtained for macrocycles **1** are in good agreement with those published for **1b**. The highest value found for **1a** decreases with increasing length of alkyl chains as the solvation of peripheral substituents competes with $\pi-\pi$ stacking of the macrocyclic cores. Glycol chains decrease the association of **1d** molecules due to their different solvation or steric demands. Self-association of **6a−c** where molecular planarity was broken drops down in $CDCl_3$ by an order of magnitude to the limits of the method with no effect of alkyl chain length; therefore, the measurements were done also in

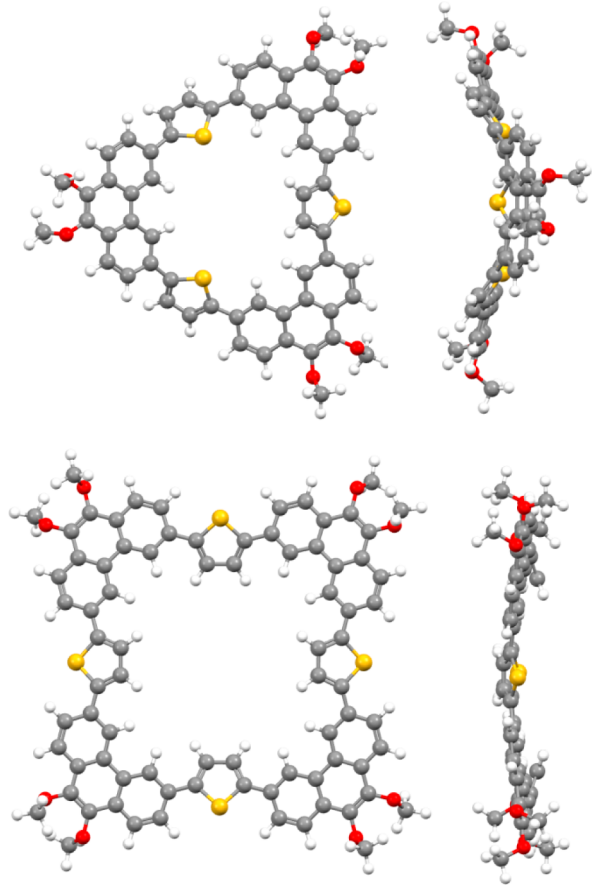

Figure 3. Computed structures of thienylene macrocycles **6a** (upper) and **7a** (bottom). The top and side views are presented.

Table 1. Association Constants[a] K_{ass} of Compounds 1, 6, and 7

compd	K_{ass} (M^{-1})	compd	K_{ass} (M^{-1})	K_{ass} (M^{-1})[c]
1a	147 ± 20	**6a**	10 ± 1	
1b	67 ± 9[b]	**6b**	10 ± 1	
1c	65 ± 1	**6c**	10 ± 0.5	9 ± 1
1d	19 ± 2	**6d**	16 ± 1	14 ± 3
1e	85 ± 3	**7c**	291 ± 33	

[a]From ^{1}H NMR measurements in $CDCl_3$ at 30 °C. Concentrations ranged from 0.3 to 20 mM except for **1a** due to its solubility and **1b** to be consistent with ref 6 (see Supporting Information). [b]Ref 6. K_{ass} = 98 ± 16 M^{-1} at 25 °C. [c]Measured in C_6D_6.

less polar benzene where a higher degree of self-association was expected, but no significant differences were found. Contrary to **1d**, glycol side chains in **6d** increase the association in comparison with the alkoxy chains. It suggests that the $\pi-\pi$ stacking governs the association of **6** much less than that of **1** and that some other effects have to be considered. The association constant of **7c** (291 ± 33 M^{-1}) does fairly correspond to the above-discussed structural considerations about the planarity of the large molecule. Dimers, trimers, and even higher assemblies were also detected by MALDI-MS spectra in samples of the macrocycles **1**, **6**, and **7** in solid state. The unique ionization and fragmentation of the molecules found in the MALDI-MS spectra are discussed elsewhere.[14]

We assumed that the association of the macrocycles in solution could be reflected also by molecular arrangement in

DOI: 10.1021/acs.joc.6b00814
J. Org. Chem. 2016, 81, 6244−6252

crystalline state; however, it was difficult to grow a single crystal suitable for X-ray diffraction. The substances either did not crystallize, or the crystals were not good enough for the measurement. A usable set of diffraction data was finally obtained for a crystal of **1e**, yet the structure solution was complicated by the high disorder of butyl chains and solvent molecules, so we had to resign on hydrogen atoms description. The structure obtained from this data set is depicted in Figure 4 and shows indeed that the molecules of **1e** are tightly associated in the dimers. The dimers are ordered in crystal as tiles in parallel overlapping layers.

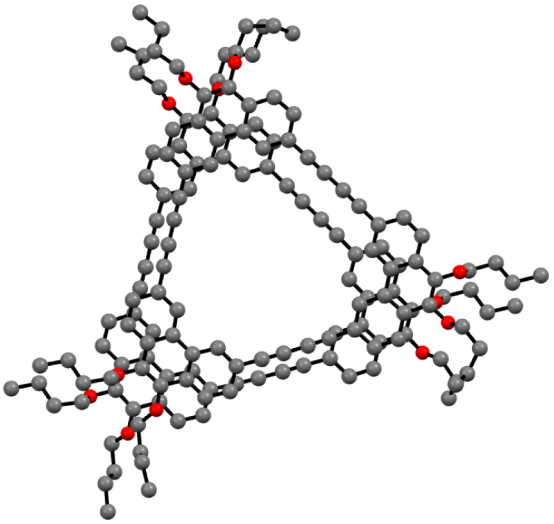

Figure 4. X-ray structure of a stacked dimer of **1e**. Hydrogen atoms and solvent molecules were omitted for clarity.

UV−vis absorption and emission spectra of the triangular macrocycles **1a−d** have the same shape with small differences in molar absorption coefficients (Table 2) which do not correlate with external chains length. Only small differences were found also in the spectra of thienylene macrocycles **6a−d** where the longer chains resulted in slightly higher absorption coefficients. This is in agreement with the literature which has studied properties of alkyl substituted dyes.[23]

In comparison with **1a−d**, the introduction of thienylene linkers to the structure resulted in a lowering of λ_{max} of **6a−d** by about 15 nm. Unlike that, there was a remarkable increase of λ_{max} (25 nm) observed in the UV−vis spectrum of **7c** compared to those for **2b** and **2c**. It does reflect different conformational behavior that enables better delocalization of π-electrons in **7c**. The absorption and emission spectra of the hexyloxy substituted macrocycles **1c**, **2c**, **6c**, and **7c** are depicted in Figure 5 for comparison; further details can be found in Supporting Information.

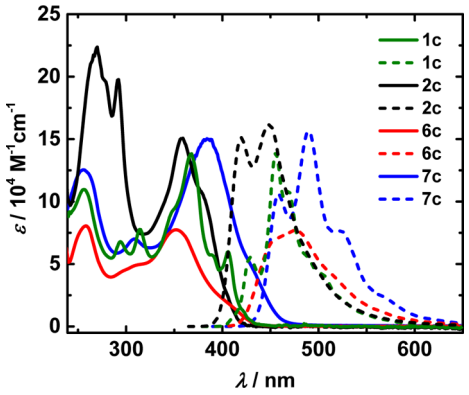

Figure 5. Comparison of UV−vis absorption and emission spectra of macrocycles **1c**, **2c**, **6c**, and **7c** in $CHCl_3$ (1×10^{-5} M).

The already mentioned redox behavior of **7c** makes obvious that the transformation of the butadiynylene linkers into the thienylene ones increases the electron donating ability of the macrocycles. It is apparent from a comparison of cyclic voltammetry (CV) curves of the macrocycles **1c**, **6c**, and **7c** (Figure 6). The reversible oxidation waves in CV of the

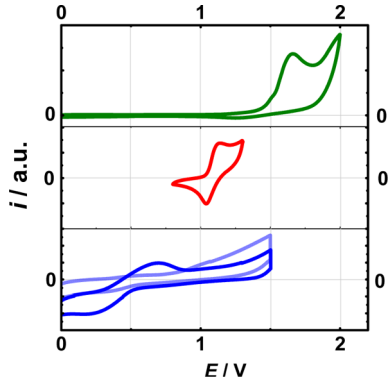

Figure 6. Comparison of the oxidation parts of cyclic voltammograms of **1c** (green), **6c** (red), and **7c** (blue/light blue) macrocycles (c = 1 mM in CH_2Cl_2) recorded at a scan rate of 100 mV/s with 0.1 M $TBAPF_6$ as the supporting electrolyte, Ag/AgCl/3 M KCl aqueous reference electrode, and platinum working and counter electrodes. The light blue curve for **7c** was obtained in the first cycle, the solid blue curve after the sample dwelt at 1.5 V potential for 8 min (for more details see SI).

compounds **6** correspond[24] to the energy of the highest occupied molecular orbital (HOMO) E_{HOMO} = −5.35 eV that is in good agreement with DFT calculations (Table 3). The methyl substituted **6a** oxidizes at slightly lower potential than the derivatives with longer chains probably due to its lower solubility and thus a higher adsorption on the electrode (for

Table 2. UV−Vis Spectral Data of Macrocycles 1a−e, 2c−d, 6a−d, and 7c

butadiynylene macrocycle	λ_{max} (nm)	$\varepsilon/10^3$ ($M^{-1}cm^{-1}$)	thienylene macrocycle	λ_{max} (nm)	$\varepsilon/10^3$ ($M^{-1}cm^{-1}$)
1a	364, 404	133.0, 28.8	**6a**	350, 407	65.5, 14.0
1b	367, 406	122.4, 52.7	**6b**	351, 407	73.4, 16.0
1c	367, 406	122.8, 60.0	**6c**	352, 407	74.2, 18.1
1d	366, 405	128.4, 30.3	**6d**	352, 407	77.3, 19.5
1e	367, 406	163.3, 53.2			
2b	357, 382	150.2, 60.0			
2c	357, 382	150.8, 101.2	**7c**	385, 431	151.0, 48.8

DOI: 10.1021/acs.joc.6b00814
J. Org. Chem. 2016, 81, 6244−6252

Table 3. Comparison of Electronic Properties of Compounds 1a, 2a, 6c, and 7c Obtained Experimentally and by Calculations

compd	calcd E_{HOMO}[a] (eV)	exp E_{HOMO}[b] (eV)	cacld E_{LUMO}[a] (eV)	calcd. gap E_g[a] (eV)	optical gap E_g[c] (eV)
1a	−5.53	−5.69	−2.41[d]	3.12	3.00
2c[e]	−5.59		−2.30	3.29	3.05
6a	−5.34	−5.31	−2.05	3.29	2.88
7c[e]	−5.22	−4.61	−2.21	3.01	2.71

[a]Calculated by DFT B3LYP/6-311++G(d,p); for more details, see Supporting Information. [b]From CV in 0.1 M *n*-Bu_4NPF_6/CH_2Cl_2 with scan rates between 50 mV/s and 100 mV/s; values were calculated using the ferrocene HOMO level: $E_{HOMO} = (E^{ox}_{onset} - E^{(1/2)}_{Fc/Fc^+} + 4.8)$ eV. [c]From UV−vis spectra as $E_g = 1242/\lambda_{onset}$. [d]From the CV measurements, $E_{LUMO} = -2.59$ eV was determined for **1c**. [e]Calculated data are for **2a** and **7a**.

more details see Supporting Information). Contrary to that, the CV measurement of **7c** was complicated by surprisingly low adsorption on the electrode, which resulted in very low sensitivity of the measurement. That was obviously the reason why there was almost no oxidation peak observed in the first scan and that also the corresponding reduction peak was very weak. It has changed slightly for repeated scans. A satisfactory result was obtained by using a modification of voltammetric stripping when a sample was allowed to dwell at potential 1.5 V in order to accumulate a sufficient concentration of the oxidation product at the electrode surface.[25] Subsequent reduction and the corresponding oxidation provided clear CV peaks. The other way to increase the low adsorption of **7c** on the electrode surface was the use of an Au-electrode. That measurement showed three separate oxidation waves (Figure 7). The HOMO energy of **7c** calculated from the onset of the

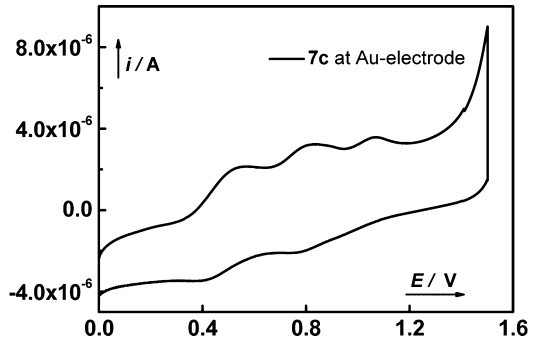

Figure 7. Cyclic voltammogram of **7c** (c = 1 mM in $CHCl_3$) with 0.1 M $TBAPF_6$ as the supporting electrolyte, Ag/AgCl/3 M KCl aqueous reference electrode, and gold and platinum working and counter electrodes, respectively, recorded at a scan rate of 100 mV/s.

first oxidation wave was −4.61 eV, which is slightly higher than the value calculated. The energy gaps between HOMO and the lowest unoccupied molecular orbital (LUMO) was estimated from the UV−vis spectra absorption edge. It is obvious that the better planarity of the macrocycles **1** and **7** results in smaller energy gaps in comparison with those of **2** and **6**. This relationship is also in good agreement with the DFT calculations.

When increasing the potential range of CV measurements, the additional irreversible oxidation waves have been observed also for **6a−d** macrocycles (Figure 8), which suggest further oxidation to the corresponding dications. For more detailed investigation of that behavior, UV−vis spectroelectrochemical measurements of the macrocycles **6c** and **7c** have been done in chloroform solution with the $TBAPF_6$ electrolyte (Figure 9). For the macrocycle **6c**, an increase of the potential from 0.9 to 1.2 V caused a decrease of absorption at 385 nm. New absorption bands appeared at 550 and 1100 nm which indicate

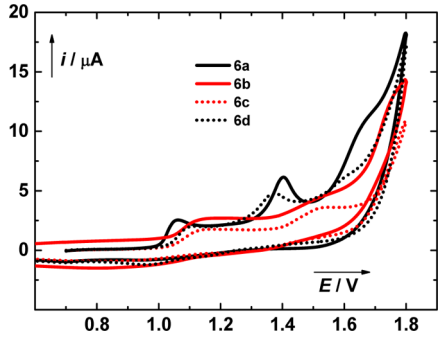

Figure 8. Comparison of cyclic voltammograms of the macrocycles **6a−d**.

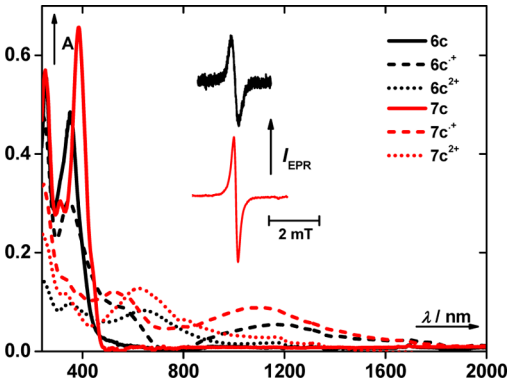

Figure 9. UV−vis spectra of **6c** and **7c** and corresponding radical cation and dication species obtained from spectroelectrochemical measurements in $CHCl_3$ ($c = 1 \times 10^{-3}$ M). Representative EPR spectra of paramagnetic species detected upon EPR spectroelectrochemical measurements are shown in insets.

the formation of a cation radical species. When the potential further increased up to 1.8 V, the absorptions at 800−1100 nm faded away, and a new absorption band was observed at 680 nm. This behavior can be rationalized by the formation of dication $\mathbf{6c}^{2+}$ by further oxidation. Similar behavior has also been observed for the tetramer **7c**; however, due to very slow diffusion the experiment setup had to be changed. The UV−vis spectroelectrochemical measurements were done at a constant potential of 2.5 V in different times. The shape of the time dependent spectra of **7c** oxidation did correspond nicely to that of the potential dependent ones obtained for the oxidation of **6c**.

Additional evidence of radical cation formation gave EPR spectroelectrochemical measurements of **6c** and **7c** which indeed detected radical species upon the first oxidation of the macrocycles. The shape of the EPR signals depicted in the insets of Figure 8 again gives evidence of better electron delocalization in $\mathbf{7c}^{\bullet+}$ than in $\mathbf{6c}^{\bullet+}$.

DOI: 10.1021/acs.joc.6b00814
J. Org. Chem. 2016, 81, 6244−6252

CONCLUSIONS

In summary, we have synthesized a series of phenanthrene-butadiynylene macrocycles decorated with external alkoxy chains of various lengths by coupling reactions of 9,10-alkoxy-3,6-diethynylphenanthrenes. Trimeric macrocycles were isolated as main products in moderate yields. Although they crystallized with difficulties, the butoxy chain derivative provided a crystal suitable for X-ray structure analysis that showed layered packing of $\pi-\pi$ stacked dimers. One representative of the tetrameric byproducts that were also formed in the coupling reactions was isolated for further investigation. Butadiyne linkers of the isolated macrocycles were transformed into the phenanthrene-thienylene ones by an addition of hydrogen sulfide. The transformation of the straight angled butadiynylene linkers to the obtuse angled thienylene ones changed the geometry of the macrocycles: the trimeric ones lost their planarity, while the tetrameric one did gain it. That influenced a self-association behavior of the macrocycles. In addition, the introduction of thiophene rings into the structure of the macrocycles decreased their oxidation potential, for the tetrameric one more than for the trimeric ones. The presence of radical cationic intermediates upon the oxidation was proved by NMR and spectroelectrochemical (UV−vis and EPR) measurements.

EXPERIMENTAL SECTION

All reactions were carried out in oven-dried glassware and under inert atmosphere unless otherwise stated. 3,6-Dibromophenanthrenequinone,[7,26] 3,6-dibromophenanthrene-9,10-diol,[27] and the compounds **4b**[7,5] and **5b**[7,5] were prepared after literature procedures. Column chromatography was carried on silica gel (230−400 mesh). IR spectra of neat compounds were recorded on an FT-IR spectrometer equipped with an ATR module with a diamond crystal. ^{1}H NMR spectra were recorded on 300 and 500 MHz spectrometers and ^{13}C NMR spectra on 75 and 125 MHz instruments in $CDCl_3$ unless stated otherwise. Chemical shifts δ in ppm were referenced to the residual signals of the solvent (δ_H = 7.26 ppm; δ_C = 77.16 ppm). UV−vis absorption and emission spectra were recorded in chloroform. MALDI-TOF measurements were done using 2,5-dihydroxy benzoic acid (DHB) and α-cyano-4-hydroxy cinnamic acid (CHCA) matrices.

3,6-Dibromo-9,10-dimethoxyphenanthrene (4a).[13] 3,6-Dibromo-9,10-phenanthrenequinone (1.00 g, 3.0 mmol), Bu_4NBr (0.38 g, 1.2 mmol), and $Na_2S_2O_4$ (4.08 g, 12 mmol) were suspended in aqueous THF (1:1, 50 mL) and stirred until the reaction mixture was homogeneous. Me_2SO_4 (2 mL) was slowly added, followed by a concentrated aq. NaOH solution (14 M, 5 mL). After stirring for 5 min, ice (20 g) was slowly added over 5 min, and the mixture was further stirred for 20 min. The resulting solid was filtered and dissolved in EtOAc (50 mL). The solution was washed with water (3 × 100 mL), dried over Na_2SO_4, filtered, and concentrated in vacuo to afford the title compound **4a** as white crystals (0.95 g, 2.33 mmol, 98%). Mp: 157.9−159.3 °C. ^{1}H NMR: δ 8.66 (d, J = 1.8 Hz, 2H); 8.07 (d, J = 8.8 Hz, 2H); 7.72 (dd, J = 8.8, 1.9 Hz, 2H); 4.07 (s, 6H). ^{13}C NMR: δ 143.8, 130.5, 128.9, 128.2, 125.4, 124.0, 120.5, 60.9.

3,6-Dibromo-9,10-bis(decyloxy)phenanthrene (4c).[7] 3,6-Dibromo-9,10-phenanthrenequinone (3.00 g, 8.20 mmol), Bu_4NBr (3.00 g, 8.20 mmol), and $Na_2S_2O_4$ (14.4 g, 82.8 mmol) were suspended in aqueous THF (1:1, 120 mL) and stirred until the reaction mixture was homogeneous. 1-Bromodecane (19.08 g, 86.0 mmol) was added followed by KOH (12.00 g, 214.0 mmol) in H_2O (60 mL). After stirring for 2 days, the reaction mixture was diluted with H_2O (200 mL) and extracted with DCM (2 × 100 mL), dried over Na_2SO_4, and concentrated in vacuo. The high boiling didecyl ether was removed by Kugelrohr distillation (125 °C 100 mTorr). Chromatography on silica gel with hexane gave the desired **4c** as white crystals (4.14 g, 6.4 mmol, 78%). Mp: 64.6−64.9 °C. ^{1}H NMR: δ 8.64 (s, 2H); 8.09 (d, J = 8.8 Hz, 2H); 7.70 (d, J = 8.7 Hz, 2H); 4.18 (t, J = 6.7 Hz, 4H); 1.93−1.83 (m, 4H); 1.59−149 (m, 4H); 1.41−129 (m, 24H); 0.89 (t, J = 6.5 Hz, 6H). ^{13}C NMR: δ 143.1, 130.4, 128.8, 128.7, 125.3, 124.2, 120.3, 73.7, 31.9, 30.4, 29.6, 29.5, 29.5, 29.3, 26.2, 22.6, 14.1. IR: 2954, 2924, 2848, 1614, 1588, 1468, 1431, 1344, 1311, 1172, 1123, 1093, 1069, 1053, 1016, 970, 912, 863, 817, 723, 615, 571, 538, 460, 420. UV−vis (2.0×10^{-5} M in $CHCl_3$) λ_{max} (log ε): 254 nm (4.75), 261 (4.79), 283 (4.34), 304 (4.20), 316 (4.22), 355 (3.08), 372 (3.12). HRMS (APCI) m/z: $[M + H]^+$ calcd for $C_{34}H_{49}Br_2O_2$ 647.2094; found 647.2103.

3,6-Dibromo-9,10-bis(2-(2-methoxyethoxy)ethoxy)-phenanthren (4d). 3,6-Dibromophenanthrene-9,10-diol[26] (1.00 g, 2.7 mmol), 1-bromo-2-(2-methoxyethoxy)ethane (1.98 g, 10.8 mmol), and K_2CO_3 (1.5 g, 10.8 mmol) were heated to 120 °C in DMF (25 mL) under N_2 atmosphere for 18 h and then cooled to room temperature. The mixture was poured into water and was extracted with DCM (3 × 80 mL). Resulting organic phases were dried over Na_2SO_4 and concentrated under reduced pressure. The residue was purified by column chromatography on silica gel (hexane/EtOAc, 3:1) to afford **4d** as white crystals (1 g, 1.75 mmol, 66%). Mp: 53.5−54.3 °C. ^{1}H NMR: δ 8.64 (d, J = 1.8 Hz, 2H); 8.24 (d, J = 8.8 Hz, 2H); 7.69 (dd, J = 8.8, 1.8 Hz, 2H); 4.41−4.38 (m, 4H); 3.85−3.82 (m, 4H); 3.70−3.67 (m, 4H), 3.59−3.56 (m, 4H); 3.40 (s, 6H). ^{13}C NMR: δ 142.8, 130.4, 128.9, 128.5, 125.2, 124.6, 120.5, 72.4, 71.9, 70.5, 70.3, 59.0. IR: 2968, 2868, 2805, 1613, 1585, 1480, 1462, 1432, 1394, 1342, 1312, 1281, 1236, 1197, 1174, 1110, 1070, 1026, 943, 919, 857, 837, 822, 810, 557, 536, 416. UV−vis (2.0×10^{-5} M in $CHCl_3$) λ_{max} (log ε): 253 nm (4.77), 261 (4.81), 282 (4.37), 302 (4.24), 315 (4.26), 353 (3.25), 372 (3.22). HRMS (APCI) m/z: $[M + H]^+$ calcd for $C_{24}H_{29}Br_2O_6$ 571.0325; found 571.0332.

3,6-Dibromo-9,10-bis(butyloxy)phenanthrene (4e). The procedure used for the preparation of **4c** was followed, and the product was isolated as white crystals (**4e**, 3.0 g, 6.2 mmol, 76%). Mp: 73.1−75.0 °C. ^{1}H NMR: δ 8.64 (d, J = 1.8 Hz, 2H); 8.09 (d, J = 8.8 Hz, 2H); 7.70 (dd, J = 8.8, 1.8 Hz, 2H); 4.19 (t, J = 6.7 Hz, 4H); 1.95−1.80 (m, 4H); 1.59 (m, 4H); 1.03 (t, J = 7.4 Hz, 6H). ^{13}C NMR: δ 143.1, 130.4, 128.8, 128.7, 125.3, 124.1, 120.2, 73.4, 32.5, 19.4, 13.9. IR: 2956, 2930, 2869, 1614, 1587, 1564, 1476, 1464, 1431, 1390, 1342, 1313, 1223, 1170, 1118, 1090, 1067, 1046, 1018, 991, 968, 943, 914, 863, 844, 813, 738, 713, 618, 566, 528. UV−vis (2.0×10^{-5} M in $CHCl_3$) λ_{max} (log ε): 253 nm (4.70), 261 (4.75), 283 (4.29), 304 (4.16), 316 (4.17). HRMS (APCI) m/z: $[M + H]^+$ calcd for $C_{22}H_{25}Br_2O_2$: 479.0216; found 479.0202.

4,4′-(9,10-Dimethoxyphenanthrene-3,6-diyl)bis(2-methylbut-3-yn-2-ol) (5a). A flame-dried flask was charged with $PdCl_2(PPh_3)_2$ (213 mg, 0.30 mmol), CuI (43 mg, 0.22 mmol), **4a** (1.5 g, 3.80 mmol), and 2-methylbut-3-yn-2-ol (1.29 g, 15.00 mmol). Dry and degassed THF (80 mL) and triethylamine (40 mL) were added via syringe. The reaction mixture had been stirred for 7 h at 70 °C and diluted with water (200 mL). The aqueous mixture was extracted with DCM (2 × 100 mL). Combined organic layers were dried over Na_2SO_4 and concentrated under reduced pressure, and the crude residue was purified by column chromatography over silica gel (DCM/EtOAc, 4:1) to afford **5a** as a yellow solid (1.4 g, 3.4 mmol, 92%). Mp: 66.1−66.8 °C. ^{1}H NMR: δ 8.64 (d, J = 1.2 Hz, 2H); 8.12 (d, J = 8.4 Hz, 2H); 7.61 (dd, J = 8.5, 1.4 Hz, 2H); 4.06 (s, 6H); 2.27 (s, 2H), 1.70 (s, 12H). ^{13}C NMR: δ 144.3, 129.8, 128.8, 127.7, 126.2, 122.1, 120.2, 94.4, 82.5, 65.7, 60.9, 31.5. IR: 3347, 2978, 2933, 1604, 1504, 1446, 1359, 1317, 1259, 1238, 1160, 1119, 1061, 984, 961, 949, 881, 827, 811, 598. UV−vis (2.0×10^{-5} M in $CHCl_3$) λ_{max} (log ε): 260 nm (4.84), 266 (4.81), 293 (4.13), 310 (4.15), 325 (4.36), 340 (4.33). HRMS (APCI/TOF) m/z: $[M + H - H_2O]^+$ calcd for $C_{26}H_{25}O_3$ 385.1798; found 385.1801.

4,4′-(9,10-Bis(decyloxy)phenanthrene-3,6-diyl)bis(2-methylbut-3-yn-2-ol) (5c). The procedure used for the preparation of **5a** was followed with **4c** (1.3 g, 1.9 mmol), and the product **5c** was isolated as a white solid (1.2 g, 1.8 mmol, 91%). Mp: 128.8−129.1 °C. ^{1}H NMR: δ 8.65 (s, 2H), 8.13 (d, J = 8.5 Hz, 2H), 7.60 (d, J = 7.7 Hz, 2H), 4.18 (t, J = 6.7 Hz, 4H), 2.26 (s, 2H), 1.93−1.84 (m, 4H), 1.70 (s, 12H), 1.59−1.49 (m, 4H), 1.41−1.29 (m, 24H), 0.89 (t, 6H). ^{13}C NMR: δ 143.7, 129.6, 129.4, 127.6, 126.2, 122.3, 120.0, 94.3, 82.6,

DOI: 10.1021/acs.joc.6b00814
J. Org. Chem. 2016, 81, 6244−6252

73.7, 65.7, 31.9, 31.5, 30.4, 29.6, 29.5, 29.5, 29.3, 26.2, 22.6, 14.0. IR: 3291, 3209, 2981, 2920, 2851, 1604, 1437, 1378, 1362, 1318, 1208, 1165, 1123, 1070, 1054, 952, 888, 823, 723, 553, 453, 419. UV−vis (2.0×10^{-5} M in $CHCl_3$) λ_{max} (log ε): 257 nm (4.80), 265 (4.75), 291 (4.09), 308 (4.11), 322 (4.32), 337 (4.30). HRMS (APCI/TOF) *m/z*: $[M + H - H_2O]^+$ calcd for $C_{44}H_{61}O_3$ 637.4615; found 637.4633.

4,4′-(9,10-Bis(2-(2-methoxyethoxy)ethoxy)phenanthrene-3,6-diyl)bis(2-methylbut-3-yn-2-ol) (5d). The procedure used for the preparation of **5a** was followed with **4d** (1.1 g, 1.9 mmol), and the product **5d** was isolated as a yellow solid (1.0 g, 1.7 mmol, 88%). ^{1}H NMR: δ 8.66 (s, 2H); 8.28 (d, J = 8.5 Hz, 2H); 7.61 (dd, J = 8.4, 1.2 Hz, 2H); 4.43−4.40 (m, 4H); 3.87−3.84 (m, 4H); 3.71−3.68 (m, 4H); 3.60−3.57 (m, 4H); 3.41 (s, 6H); 1.70 (s, 12H). ^{13}C NMR: δ 143.4, 129.7, 129.3, 127.8, 126.1, 122.8, 120.3, 94.4, 82.6, 72.4, 72.0, 70.5, 70.5, 65.7, 59.1, 31.5. IR: 3405, 2978, 2874, 1603, 1503, 1436, 1351, 1317, 1258, 1105, 1062, 962, 944, 879, 830, 556. UV−vis (2.0×10^{-5} M in $CHCl_3$) λ_{max} (log ε): 261 nm (4.85), 266 (4.81), 293 (4.14), 310 (4.16), 325 (4.37), 341(4.32). HRMS (APCI/TOF) *m/z*: $[M + H - H_2O]^+$ calcd for $C_{34}H_{41}O_7$ 561.2847; found 561.2848.

4,4′-(9,10-Bis(butyloxy)phenanthrene-3,6-diyl)bis(2-methylbut-3-yn-2-ol) (5e). The procedure used for the preparation of **5a** was followed with **4e** (1.2 g, 2.4 mmol), and the product **5e** was isolated as a yellow solid (1.1 g, 2.3 mmol, 90%). ^{1}H NMR: δ 8.64 (s, 2H); 8.13 (d, J = 8.5 Hz, 2H); 7.60 (dd, J = 8.5, 1.3 Hz, 2H; 4.19 (t, J = 6.7 Hz, 4H); 2.26 (s, 2H), 1.96−1.81 (m, 4H), 1.70 (s, 12H); 1.65−1.53 (m, 4H); 1.02 (t, J = 7.4 Hz, 6H). ^{13}C NMR: δ 143.6, 129.6, 129.4, 127.6, 126.2, 122.3, 120.0, 94.3, 82.6, 73.4, 65.7, 32.5, 31.5, 19.4, 13.9. IR: 3340, 2957, 2931, 2871, 1603, 1554, 1503, 1456, 1435, 1356, 1316, 1260, 1206, 1164, 1119, 1065, 1046, 1019, 961, 945, 910, 883, 826, 752, 714, 682, 619, 596, 555, 517. UV−vis (2.0×10^{-5} M in $CHCl_3$) λ_{max} (log ε): 260 nm (4.80), 267 (4.78), 293 (4.05), 311 (4.08), 326 (4.31), 342 (4.28). HRMS (APCI/TOF) *m/z*: $[M + H - H_2O]^+$ calcd for $C_{32}H_{37}O_3$ 469.2737; found 469.2736.

3,6-Diethynyl-9,10-dimethoxyphenanthrene (3a). Powdered KOH (1.00 g, 19.0 mmol) was added to a solution of compound **5a** (1.3 g, 3.2 mmol) in benzene (80 mL) and refluxed for 1 h. After cooling to room temperature, the reaction mixture was filtered through a short pad of a silica gel to afford **3a** as a yellow solid (0.8 g, 2.7 mmol 85%). Mp: 126.1−127.6 °C. ^{1}H NMR: δ 8.75 (s, 2H); 8.18 (d, J = 8.5 Hz, 2H); 7.71 (dd, J = 8.4, 1.1 Hz, 2H); 4.08 (s, 6H); 3.21 (s, 2H). ^{13}C NMR: δ 144.5, 130.1, 129.3, 127.6, 126.9, 122.3, 119.7, 84.0, 77.8, 60.9. IR: 3263, 2971, 2936, 2837, 1603, 1318, 1119, 1058, 981, 877, 826, 657, 635, 610, 598, 556, 539, 486. UV−vis (2.0×10^{-5} M in $CHCl_3$) λ_{max} (log ε): 257 nm (4.80), 265 (4.75), 291 (4.09), 308 (4.11), 322 (4.32), 337 (4.30), 374 (3.02). HRMS (APCI/TOF) *m/z*: $[M + H]^+$and $[2\ M + H]^+$ calcd for $C_{20}H_{15}O_2$ 287.1066 and for $C_{40}H_{29}O_4$ 573.2060; found 287.1067 and 573.2066.

9,10-Bis(hexyloxy)3,6-diethynylphenanthrene (3b).[5,12] The procedure used for the preparation of **3a** was followed with **5b** (1.9 g, 3.5 mmol), and the product **3b** was isolated as a yellow solid (1.0 g, 2.3 mmol, 66%). ^{1}H NMR: δ 8.75 (d, J = 1.5 Hz, 2H); 8.18 (d, J = 8.5 Hz, 2H); 7.70 (dd, J = 8.5, 1.4 Hz, 2H); 4.20 (t, J = 6.7 Hz, 4H); 3.21 (s, 2H); 2.17−1.76 (m, 4H); 1.74−1.44 (m, 4H); 1.46−1.25 (m, 8H); 0.94 (t, J = 5.8, 2.9 Hz, 6H). ^{13}C NMR: δ 143.8, 130.0, 129.8, 127.6, 126.9, 122.5, 119.5, 84.1, 77.7, 73.7, 31.6, 30.4, 25.8, 22.6, 14.0. HRMS (APCI/TOF) *m/z*: $[M + H]^+$ calcd for $C_{30}H_{35}O_2$ 427.2632; found 427.2631).

9,10-Bis(decyloxy)3,6-diethynylphenanthrene (3c). The procedure used for the preparation of **3a** was followed with **5c** (1.5 g, 2.2 mmol), and the product **3c** was isolated as a yellow solid (0.8 g, 1.4 mmol, 65%). Mp: 60.5−61.1 °C. ^{1}H NMR: δ 8.75 (s, 2H); 8.18 (d, J = 8.5 Hz, 2H); 7.69 (d, J = 8.5 Hz, 2H); 4.19 (t, J = 6.7 Hz, 4H); 3.20 (s, 2H); 1.94−1.85 (m, 4H); 1.59−1.50 (m, 4H); 1.41−1.29 (m, 24H); 0.91 (t, 6H). ^{13}C NMR: δ 143.9, 130.0, 129.9, 127.6, 126.9, 122.5, 119.5, 84.1, 77.7, 73.7, 31.9, 30.4, 29.6, 29.5, 29.5, 29.3, 26.2, 22.6, 14.0. IR: 3284, 2917, 2848, 1605, 1465, 1437, 1321, 1238, 1174, 1120, 1070, 1056, 882, 820, 719, 674, 658, 612, 597, 577. UV−vis (2.0×10^{-5} M in $CHCl_3$) λ_{max} (log ε): 257 nm (4.89), 265 (4.84), 275 (4.55) 291 (4.17), 309 (4.16), 324 (4.38), 339 (4.36). HR-MS (APCI/TOF) *m/z*: $[M + H]^+$, $[2\ M + H]^+$ calcd for $C_{38}H_{51}O_2$ 539.3883 and for $C_{76}H_{101}O_4$ 1077.7694; found 539.3892 and 1077.7708.

9,10-Bis(2-(2-methoxyethoxy)ethoxy)-3,6-diethynylphenanthrene (3d). The procedure used for the preparation of **3a** was followed with **5d** (1.0 g, 1.7 mmol), and the product **3d** was isolated as a yellow solid (0.5 g, 1.0 mmol, 62%). ^{1}H NMR: δ 8.74 (s, 2H); 8.31 (d, J = 8.5 Hz, 2H); 7.68 (d, J = 8.5 Hz, 2H); 4.43−4.40 (m, 4H); 3.87−3.84 (m, 4H); 3.71−3.68 (m, 4H); 3.60−3.57 (m, 4H); 3.40 (s, 6H); 3.20 (s, 2H). ^{13}C NMR: δ 143.5, 130.0, 129.6, 127.0, 126.7, 122.8, 119.6, 84.0, 77.7, 72.4, 71.9, 70.5, 70.4, 59.0. IR: 3252, 2876, 1603, 1435, 1344, 1318, 1237, 1133, 1103, 1065, 1045, 1024, 938, 872, 848, 834, 821, 624, 577, 539. UV−vis (2.0×10^{-5} M in $CHCl_3$) λ_{max} (log ε): 257 nm (4.85), 265 (4.79), 291 (4.12), 308 (4.13), 323 (4.35), 337 (4.32). HRMS (APCI) *m/z*: $[M + H]^+$ calcd for $C_{28}H_{31}O_6$ 463.2115; found 463.2124.

9,10-Bis(butyloxy)3,6-diethynylphenanthrene (3e). The procedure used for the preparation of **3a** was followed with **5e** (1.7 g, 3.4 mmol), and the product **3e** was isolated as a yellow solid (**3e**, 0.9 g, 2.4 mmol, 70%). ^{1}H NMR: δ 8.75 (s, 2H), 8.18 (d, J = 8.5 Hz, 2H), 7.70 (d, J = 9.7 Hz, 2H), 4.21 (t, J = 6.7 Hz, 4H), 3.21 (s, 2H), 1.85 (m, 4H), 1.59 (m, 4H), 1.03 (t, J = 7.4 Hz, 6H). ^{13}C NMR: δ 143.8, 130.0, 129.8, 127.6, 126.91, 122.4, 119.5, 84.1, 77.72, 73.4, 32.5, 19.4, 13.9. IR: 3293, 2957, 2930, 2870, 1603, 1555, 1501, 1457, 1434, 1378, 1352, 1315, 1261, 1235 1171, 1119, 1091, 1065, 1046, 1019, 992, 963, 945, 913, 883, 864, 827, 815, 738, 714, 646, 618, 595, 568, 529. UV−vis (2.0×10^{-5} in $CHCl_3$) λ_{max} (log ε): 257 nm (4.82), 266 (4.78), 291 (4.10), 311 (4.12), 323 (4.33), 338 (4.30), 374 (2.58). HRMS (APCI) *m/z*: $[M+1]^+$ calcd for $C_{26}H_{27}O_2$ 371.2006; found 371.

General Procedure for Synthesis of the Macrocycles 1a−e and 2b−c. A 500 mL flask was charged with $PdCl_2(PPh_3)_2$ (8 mol %) and CuI (6 mol %), and suitable aromatic diyne, THF (150 mL), and triethylamine (150 mL) were added, and the reaction mixture was stirred overnight at room temperature under air atmosphere. The solvent was removed, and the residual material was purified by column chromatography over silica gel.

Macrocycle ***1a.*** 60 mg, 30%, yellow solid. Mp: > 300 °C. ^{1}H NMR: δ 8.59 (s, 6H); 7.94 (d, J = 8.5 Hz, 6H); 7.57−7.49 (m, 6H); 4.05 (s, 18H). ^{13}C NMR: δ 144.3, 129.5, 128.9, 127.4, 127.1, 121.9, 119.4, 82.5, 75.2, 60.8. IR: 2920, 2850, 1723, 1601, 1551, 1506, 1444, 1417, 1366, 1316, 1238, 1200, 1119, 1063, 984, 876, 818, 593, 541. UV−vis (1.0×10^{-5} in $CHCl_3$) λ_{max} (log ε): 257 nm (4.78), 292 (4.59), 313(4.55), 344 (4.59), 366 (4.78), 388 (4.38), 404 (4.40). MALDI-TOF-MS (CHCA) *m/z*: $[M]^+$ calcd for $C_{60}H_{36}O_6$ 852.2512; found 852.257 (see the Supporting Information for theoretical and experimental isotopic distributions).

Macrocycle ***1b.*** 77 mg, 39%, yellow solid. Mp: 227.5−230.9 °C. ^{1}H NMR: δ 8.60 (d, J = 1.7 Hz, 6H), 7.94 (d, J = 8.5 Hz, 6H), 7.53 (dd, J = 8.5, 1.3 Hz, 6H), 4.15 (t, J = 6.7 Hz, 12H), 1.95−1.85 (m, 12H), 1.63−1.56 (m, 12H), 1.45−1.40 (m, 24H), 0.99−0.95 (m, 18H). ^{13}C NMR: δ 143.9, 129.6, 129.5, 127.5, 127.2, 122.2, 119.2, 82.6, 75.1, 73.6, 31.8, 30.5, 25.9, 22.7, 14.0. IR: 2923, 2854, 1600, 1505, 1464, 1433, 1379 1314, 1235, 1173, 1121, 1050, 990, 925, 878, 822, 723, 623, 887, 539. UV−vis (1.0×10^{-5} M in $CHCl_3$) λ_{max} (log ε): 256 nm (4.99), 294 (4.77), 314(4.82), 347 (4.90), 367 (5.07), 390 (4.70), 407 (4.71). MALDI-TOF-MS (CHCA) *m/z*: $[M]^+$ calcd for $C_{90}H_{96}O_6$ 1272.7206; found 1272.725 (see the Supporting Information for theoretical and experimental isotopic distributions).

Macrocycle ***1c.*** 84 mg, 42%, yellow solid. ^{1}H NMR: δ 8.65 (s, 6H); 8.00 (d, J = 8.5 Hz, 6H); 7.58 (dd, J = 8.5, 1.4 Hz, 6H); 4.16 (t, J = 6.6 Hz, 12H); 1.93−1.84 (m, 12H); 1.63−1.53 (m, 12H); 1.48−1.29 (m, 72H); 0.95−0.91 (m, 18H). ^{13}C NMR: δ 143.7, 129.3, 129.1, 127.4, 127.0, 121.9, 119.2, 82.6, 75.3, 73.6, 31.9, 30.6, 29.7, 29.7, 29.4, 26.3, 22.7, 14.1. IR: 2920, 2851, 1601, 1506, 1464, 1434, 1360, 1315, 1261, 1236, 1173, 1122, 1052, 976, 878, 822, 719, 624, 588, 540. UV−vis (1.0×10^{-5} M in $CHCl_3$) λ_{max} (log ε): 257 nm (5.02), 294 (4.82), 314(4.88), 346 (5.01), 347 (4.95), 367 (5.13), 390 (4.75), 407 (4.77). MALDI-TOF-MS (CHCA) *m/z*: $[M]^+$ calcd for $C_{114}H_{144}O_6$: 1610.0962; found 1610.099 (see the Supporting Information for theoretical and experimental isotopic distributions).

DOI: 10.1021/acs.joc.6b00814
J. Org. Chem. 2016, 81, 6244−6252

Macrocycle ***1d***. 70 mg, 35%, yellow solid. Mp: 120.1−121.0 °C. ^{1}H NMR: δ 8.69 (s, 6H); 8.21 (d, J = 8.5 Hz, 6H); 7.63 (d, J = 8.5 Hz, 6H); 4.46−4.40 (m, 12H); 3.89−3.87 (m, 12H); 3.73−7.70 (m, 12H); 3.62−3.59 (m, 12H); 3.43 (s, 18H). ^{13}C NMR: δ 143.7, 129.7, 129.5, 127.4, 127.4, 122.8, 119.4, 82.5, 75.0, 72.5, 72.0, 70.5, 70.5, 59.1. IR: 2916, 2850, 1730, 1601, 1434, 1350, 1318, 1239, 1196, 1179, 1104, 1064, 937, 923, 877, 818, 718, 624, 540. UV−vis (1.0×10^{-5} in $CHCl_3$) λ_{max} (log ε): 257 nm (4.88), 293 (4.68), 314(4.69), 346 (4.76), 366 (4.93), 389 (4.57), 404 (4.58). MALDI-TOF-MS (CHCA) m/z: $[M + Na]^+$ calcd for $C_{84}H_{84}NaO_{18}$: 1403.5550; found 1403.553 (see the Supporting Information for theoretical and experimental isotopic distributions).

Macrocycle ***1e***. 84 mg, 42%, yellow solid. Mp: > 300 °C. ^{1}H NMR: δ 8.71 (s, 6H); 8.08 (d, J = 8.5 Hz, 6H); 7.65 (d, J = 8.5 Hz, 6H); 4.20 (t, J = 6.5 Hz, 12H); 1.90 (p, J = 7.0 Hz, 12H); 1.62 (q, J = 7.5 Hz, 12H); 1.06 (t, J = 7.3 Hz, 18H). ^{13}C NMR: δ 143.8, 129.3, 127.4, 127.11, 122.0, 119.2, 82.6, 75.2, 73.2, 32.6, 19.5, 14.0. IR: 2955, 2928, 2869, 1689, 1598, 1525, 1505, 1431, 1413, 1357, 1330, 1314, 1234, 1172, 1115, 1063, 1044, 964, 945, 910, 876, 819, 739, 661, 586, 539. UV−vis (2.0×10^{-5} M in $CHCl_3$) λ_{max} (log ε): 256 nm (4.97), 294 (4.68), 314 (4.79), 347 (4.85), 367 (5.07), 390 (4.64), 407 (4.71). HRMS (APCI) m/z: $[M + H]^+$ calcd for $C_{78}H_{73}O_6$ 1105.5401; found 1105.5387.

Macrocycle ***2b***. 22 mg, 12% yellow solid. ^{1}H NMR: δ 8.81 (s, 8H); 8.17 (d, J = 8.5 Hz, 8H); 7.73 (d, J = 8.6 Hz, 8H); 4.19 (t, J = 6.7 Hz, 16H); 1.84−1.84 (m, 16H); 1.61−1.51 (m, 16H); 1.43−1.34 (m, 16H); 1.29−1.23 (m, J = 8.5 Hz, 32H); 0.93 (t, J = 7.0 Hz, 3H). ^{13}C NMR: δ 144.2, 130.4, 130.1, 127.6, 127.4, 122.6, 119.2, 82.3, 74.8, 73.8, 31.7, 30.4, 25.8, 22.6, 14.0. IR: 2925, 2855, 2206, 2143, 1598, 1550, 1503, 1464, 1432, 1378, 1359, 1313, 1232, 1172, 1120, 1050, 988, 925, 878, 824, 783, 620, 587. UV−vis (1.0×10^{-5} M in $CHCl_3$) λ_{max} (log ε): 269 nm (5.12), 279 (5.06), 291 (5.06), 357 (4.95), 382 (4.77). MALDI-TOF-MS (CHCA) m/z: $[M]^+$ calcd for $C_{120}H_{128}O_8$ 1696.9609; found 1696.957 (see the Supporting Information for theoretical and experimental isotopic distributions).

Macrocycle ***2c***. 24 mg, 12%, yellow solid. ^{1}H NMR (500 MHz): δ 8.80 (s, 8H); 8.16 (d, J = 8.5 Hz, 8H); 7.73 (d, J = 8.6 Hz, 8H); 4.18 (t, J = 6.6 Hz, 16H); 1.91−1.84 (m, 16H); 1.59−1.50 (m,16H); 1.43−1.29 (m, 96H); 0.89 (t, J = 6.3 Hz, 24H). ^{13}C NMR: δ 144.3, 130.6, 130.2, 127.7, 127.5, 122.7, 119.5, 82.5, 74.9, 73.9, 32.1, 30.6, 29.8, 29.8, 29.7, 29.5, 26.4, 22.8, 14.2. IR: 2925, 2855, 2206, 1598, 1550, 1503, 1464, 1432, 1378, 1359, 1313, 1232, 1172, 1120, 1050, 988, 925, 878, 824, 783, 656, 587. UV−vis (1.0×10^{-5} M in $CHCl_3$) λ_{max} (log ε): 270 nm (5.34), 279 (5.29), 291 (5.29), 358 (5.17), 382 (5.00). MALDI-TOF-MS (CHCA) m/z: $[M]^+$ calcd for $C_{152}H_{192}O_8$ 2145.4611; found 2145.457 (see the Supporting Information for theoretical and experimental isotopic distributions).

General Procedure for Synthesis of Thienylene Macrocycles. To a solution of macrocycle **1** in toluene and 2-methoxyethanol (10 mL, 1:1), $Na_2S{\cdot}9H_2O$ (9 equiv) was added. The mixture was degassed with N_2, then refluxed overnight at 150 °C. The solvent was removed, and the residual material was purified by column chromatography over silica gel.

Thiophene Macrocycle ***6a***. 116 mg, 50%, yellow solid. Mp: > 300 °C.^{1}H NMR: δ 8.77 (s, 6H); 8.29 (d, J = 8.4 Hz, 1H); 7.87 (d, J = 8.5 Hz, 6H); 7.42 (s, 6H); 4.13 (s, 18H). ^{13}C NMR: δ 145.0, 143.7, 132.4, 128.8, 128.5, 126.5, 125.9, 122.5, 120.1, 61.9. IR: 2936, 2840, 1605, 1559, 1510, 1447, 1426, 1369, 1319, 1296, 1250, 1203, 1119, 1063, 988, 939, 898, 870, 815, 789, 554. UV−vis (1.0×10^{-5} M in $CHCl_3$) λ_{max} (log ε): 258 nm (4.86), 351 (4.81), 407 (4.29). MALDI-TOF-MS (CHCA) m/z: $[M]^+$ calcd for $C_{60}H_{42}O_6S_3$ 954.2138; found 954.211 (see the Supporting Information for theoretical and experimental isotopic distributions).

Thienylene Macrocycle ***6b***. 108 mg, 50%, yellow solid. ^{1}H NMR: δ 8.79 (s, 6H); 8.31 (d, J = 8.6 Hz, 6H); 7.88 (dd, J = 8.6, 1.4 Hz, 6H); 7.43 (s, 6H); 4.27 (t, J = 6.7 Hz, 3H); 2.01−1.92 (m, 12H); 1.67−1.59 (m, 12H); 1.47−1.41 (m, 12H); 1.31−1.27 (m, 36H); 0.97 (t, J = 7.0 Hz, 18H). ^{13}C NMR: δ 145.3, 143.2, 132.5, 129.3, 128.9, 126.7, 126.1, 122.9, 120.5, 73.8, 31.7, 30.5, 25.9, 22.6, 14.0. IR: 2921, 2852, 1718, 1611, 1558, 1508, 1461, 1435, 1358, 1319, 1297, 1213, 1200, 1179, 1126, 1054, 927, 880, 829, 800, 710, 622, 593, 534. UV−vis (1.0×10^{-5} M in $CHCl_3$) λ_{max} (log ε): 258 nm (4.89), 351 (4.86), 407 (4.29). MALDI-TOF-MS (CHCA) m/z: $[M + H]^+$ calcd for $C_{90}H_{102}O_6S_3$ 1374.6833; found 1374.681 (see the Supporting Information for theoretical and experimental isotopic distributions).

Thienylene Macrocycle ***6c***. 108 mg, 51%, yellow solid. ^{1}H NMR: δ 8.77 (s, 6H); 8.30 (d, J = 8.6 Hz, 6H); 7.86 (dd, J = 8.6, 1.4 Hz, 6H); 7.42 (s, 6H); 4.25 (t, J = 6.7 Hz, 12H); 1.99−1.90 (m, 12H); 1.64−1.55 (m, 12H); 1.45−1.26 (m, 72H); 0.9 (t, J = 7.0 Hz, 18H). ^{13}C NMR: δ 145.3, 143.2, 132.5, 129.3, 128.8, 126.6, 126.0, 122.9, 120.4, 73.7, 31.9, 30.5, 29.7, 29.6, 29.6, 29.3, 26.3, 22.7, 14.1. IR: 2921, 2851, 1716, 1606, 1558, 1508, 1459, 1435, 1356, 1319, 1258, 1172, 1179, 1122, 1053, 979, 925, 876, 823, 798, 719, 620, 587, 535. UV−vis (1.0×10^{-5} M in $CHCl_3$) λ_{max} (log ε): 258 nm (4.91), 352 (4.88), 407 (4.29). MALDI-TOF-MS (CHCA) m/z: $[M]^+$ calcd for $C_{114}H_{150}O_6S_3$ 1711.0589; found 1711.060 (see the Supporting Information for theoretical and experimental isotopic distributions).

Thienylene Macrocycle ***6d***. 105 mg, 50%, yellow solid. ^{1}H NMR: δ 8.77 (s, 6H); 8.43 (d, J = 8.6 Hz, 6H); 7.86 (dd, J = 8.6, 1.3 Hz, 6H); 7.43 (s, 6H); 4.49−4.46 (m, 12H); 3.93−3.90 (m, 12H); 3.77−3.74 (m, 12H); 3.65−3.61 (m, 12H); 3.43 (s, 18H). ^{13}C NMR: δ 145.3, 142.9, 132.7, 129.1, 128.9, 126.7, 126.1, 123.3, 120.3, 72.4, 72.0, 70.5, 59.1. IR: 2921, 2853, 1717, 1669, 1559, 1503, 1464, 1435, 1349, 1319, 1247, 1197, 1104, 1061, 923, 869, 824, 798, 714, 526. UV−vis (1.0×10^{-5} M in $CHCl_3$) λ_{max} (log ε): 258 nm (4.91), 351 (4.86), 407 (4.29). MALDI-TOF-MS (CHCA) m/z: $[M]^+$ calcd for $C_{84}H_{90}O_{18}S_3$: 1482.5284; found 1482.528 (see the Supporting Information for theoretical and experimental isotopic distributions).

Thienylene Macrocycle ***7c***. 105 mg, 50%, yellow solid. ^{1}H NMR: δ 8.43 (s, 6H); 7.74 (d, J = 8.2 Hz, 6H); 7.56 (s, 6H); 6.88 (d, J = 7.7 Hz, 6H); 4.24 (t, J = 6.0 Hz, 16H), 2.05−1.90 (m, 16H); 1.80−1.59 (m, 16H); 1.62−1.28 (m, 62H); 0.95 (t, J = 6.6 Hz, 24H). ^{13}C NMR: δ 143.5, 143.2, 130.2, 128.3, 128.2, 123.9, 122.2, 122.0, 116.9, 73.7, 32.25, 31.0, 30.1, 30.0, 29.7, 26.7, 22.9, 14.3. IR: 2920, 2851, 1604, 1558, 1514, 1463, 1434, 1350, 1312, 1247, 1178, 1122, 1056, 985, 939, 866, 816, 780, 719, 622. UV−vis (1.0×10^{-5} M in $CHCl_3$) λ_{max} (log ε): 256 nm (5.09), 309 (4.84), 385 (5.17), 431 (4.67). MALDI-TOF-MS (CHCA) m/z: $[M]^+$ calcd for $C_{152}H_{200}O_8S_4$: 2281.4120; found 2281.409 (see the Supporting Information for theoretical and experimental isotopic distributions).

Cyclic Voltammetry and Spectroelectrochemistry. Cyclic voltammetry measurements were performed with 1 mM samples of the macrocycles in dichloromethane with 0.1 M tetrabutylammonium hexafluorophosphate ($TBAPF_6$) as the supporting electrolyte with the Ag/AgCl/3 M KCl aqueous reference electrode separated from the main electrolytic compartment by a fritted junction. A platinum electrode (7.1 mm^2) or Au-wire was used as the working electrode, and a platinum wire was used as the counter electrode in conventional three-electrode voltammetric arrangement. UV−vis spectroelectrochemical studies were carried out under argon atmosphere with compounds dissolved in chloroform ($c = 1 \times 10^{-3}$ M) with $TBAPF_6$ (0.1 M) as a supporting electrolyte with a scan rate of 10 mV/s. The measurements were carried out in an optically transparent thin-layer electrochemical (OTTLE) cell (0.1 mm optical length, CaF_2 windows). A Pt mini-grid working electrode, Pt mini-grid reference electrode, and silver wire pseudoreference electrodes were used. EPR spectroelectrochemical measurements were performed under an argon atmosphere in the optical EPR cavity with an EMX X-band CW spectrometer.

■ ASSOCIATED CONTENT

Supporting Information

The Supporting Information is available free of charge on the ACS Publications website at DOI: 10.1021/acs.joc.6b00814.

Copies of ^{1}H and ^{13}C NMR spectra of all new compounds; calculation of self-association constants, UV−vis absorption and emission spectra, cyclic voltammetry details, DFT calculations, and X-ray

DOI: 10.1021/acs.joc.6b00814
J. Org. Chem. 2016, 81, 6244−6252

structure details; and comparison of calculated and experimental MS isotopic distributions of prepared macrocycles (PDF)

X-ray crystallographic data for compound **1e** (CIF)

AUTHOR INFORMATION

Corresponding Author

*E-mail: mazal@chemi.muni.cz.

Notes

The authors declare no competing financial interest.

ACKNOWLEDGMENTS

We are indebted to F. Amato, V. Roblová, and J. Havel for MALDI-MS measurements, I. Pilařová, L. Trnková for help with CV measurements, T. Slanina for UV−vis spectroelectrochemical measurements, and K. Luspai (STU Bratislava, Slovakia) for EPR spectroelectrochemical measurements. Computational resources were provided by the CESNET LM2015042 and the CERIT Scientific Cloud LM2015085, under the program "Large Research, Development, and Innovations Infrastructures". This research has been supported by the Ministry of Education, Youth and Sports of the Czech Republic under the project CEITEC 2020 (LQ1601). We acknowledge the CF X-ray diffraction and Bio-SAXS supported by the CIISB research infrastructure (LM2015043). S.K.M. is an international research fellow of the Japan Society for the Promotion of Science

REFERENCES

(1) (a) Jin, Y.; Wang, Q.; Taynton, P.; Zhang, W. *Acc. Chem. Res.* **2014**, *47*, 1575−1586. (b) Pasini, D. *Molecules* **2013**, *18*, 9512−9530. (c) Ong, W. Q.; Zeng, H. *J. Inclusion Phenom. Mol. Recognit. Chem.* **2013**, *76*, 1−11. (d) Fu, H.; Liu, Y.; Zeng, H. *Chem. Commun.* **2013**, *49*, 4127−4144. (e) Höger, S. *Pure Appl. Chem.* **2010**, *82*, 821−830. (f) Zhang, W.; Moore, J. *Angew. Chem., Int. Ed.* **2006**, *45*, 4416−4439. (g) Zhao, D.; Moore, J. *Chem. Commun.* **2003**, 807−818.

(2) For reviews on syntheses strategies, see: (a) Höger, S. In *Functional Organic Materials*; Müller, T. J. J., Bunz, U. H. F., Eds.; Wiley-VCH: Weinheim, Germany, 2007; p 225. (b) Sadowy, A. L.; Tykwinski, R. R. In *Modern Supramolecular Chemistry. Strategies for Macrocyclic Synthesis*; Diederich, F., Stang, P. J., Tykwinski, R. R., Eds.; Wiley-VCH: Weinheim, Germany, 2008; p 185. (c) Gross, D. E.; Zang, L.; Moore, J. S. *Pure Appl. Chem.* **2012**, *84*, 869−1112. (d) Iyoda, M.; Yamakawa, J.; Rahman, M. J. *Angew. Chem., Int. Ed.* **2011**, *50*, 10522−10553.

(3) (a) Kim, J.-J.; Kwak, O. K.; Park, J. K.; Min, K. S.; Yoon, Y.-J. *J. Inclusion Phenom. Macrocyclic Chem.* **2014**, *79*, 495−502. (b) Maran, U.; Britt, D.; Fox, C. B.; Harris, J. M.; Orendt, A. M.; Conley, H.; Davis, R.; Hlady, V.; Stang, P. J. *Chem. - Eur. J.* **2009**, *15*, 8566−8577. (c) Das, N.; Ghosh, A.; Arif, A. M.; Stang, P. J. *Inorg. Chem.* **2005**, *44*, 7130−7137. (d) Addicott, C.; Das, N.; Stang, P. J. *Inorg. Chem.* **2004**, *43*, 5335−5338. (e) Chi, K.-W.; Addicott, C.; Stang, P. J. *J. Org. Chem.* **2004**, *69*, 2910−2912. (f) Mukherjee, P. S.; Das, N.; Kryschenko, Y. K.; Arif, A. M.; Stang, P. J. *J. Am. Chem. Soc.* **2004**, *126*, 2464−2473.

(4) Smith, M. K.; Goldberg, A. R.; Northrop, B. H. *Eur. J. Org. Chem.* **2015**, *2015*, 2928−2941.

(5) Boden, B. N.; Hui, J. K.; MacLachlan, M. J. *J. Org. Chem.* **2008**, *73*, 8069−8072.

(6) He, Z.; Xu, X.; Zheng, X.; Ming, T.; Miao, Q. *Chem. Sci.* **2013**, *4*, 4525−4531.

(7) Kaleta, J.; Mazal, C. *Org. Lett.* **2011**, *13*, 1326−1329.

(8) (a) Iyoda, M.; Shimizu, H. *Chem. Soc. Rev.* **2015**, *44*, 6411−6424. (b) Huang, S.; Zou, L.-Y.; Ren, A.-M.; Zhao, Y.; Liu, X.-T.; Guo, J.-F.; Feng, J.-K. *Dyes Pigm.* **2012**, *93*, 1519−1531. (c) Iyoda, M. *Pure Appl. Chem.* **2010**, *82*, 831−841.

(9) (a) Iyoda, M.; Tanaka, K.; Shimizu, H.; Hasegawa, M.; Nishinaga, T.; Nishiuchi, T.; Kunugi, Y.; Ishida, T.; Otani, H.; Sato, H.; Inukai, K.; Tahara, K.; Tobe, Y. *J. Am. Chem. Soc.* **2014**, *136*, 2389−2396. (b) Wang, C.; Dong, H.; Hu, W.; Liu, Y.; Zhu, D. *Chem. Rev.* **2012**, *112*, 2208−2267. (c) Klauk, H. *Chem. Soc. Rev.* **2010**, *39*, 2643−2666. (d) Yamashita, Y. *Sci. Technol. Adv. Mater.* **2009**, *10*, 024313. (e) Reddy, J. S.; Anand, V. G. *J. Am. Chem. Soc.* **2009**, *131*, 15433−15439. (f) Höger, S. *Chem. - Eur. J.* **2004**, *10*, 1320−1329. (g) Dimitrakopoulos, C. D.; Malenfant, P. R. L. *Adv. Mater.* **2002**, *14*, 99−117.

(10) Garcia, M.; Ramos, E.; Guadarrama, P.; Fomine, S. *J. Phys. Chem. A* **2009**, *113*, 2953−2960.

(11) Zhang, L.; Hughes, D. L.; Cammidge, A. N. *J. Org. Chem.* **2012**, *77*, 4288−4297.

(12) (a) Li, T.; Yue, K.; Yan, Q.; Huang, H.; Wu, H.; Zhu, N.; Zhao, D. *Soft Matter* **2012**, *8*, 2405−2415. (b) Bhaskar, A.; Ramakrishna, G.; Hagedorn, K.; Varnavski, O.; Mena-Osteritz, E.; Baeuerle, P.; Goodson, T., III *J. Phys. Chem. B* **2007**, *111*, 946−954. (c) Bhaskar, A.; Guda, R.; Haley, M. M.; Goodson, T., III. *J. Am. Chem. Soc.* **2006**, *128*, 13972−13973. (d) Seo, S. H.; Jones, T. V.; Seyler, H.; Peters, J. O.; Kim, T. H.; Chang, J. Y.; Tew, G. N. *J. Am. Chem. Soc.* **2006**, *128*, 9264−9265.

(13) (a) Li, J.; Hu, G.; Wang, N.; Hu, T.; Wen, Q.; Lu, P.; Wang, Y. *J. Org. Chem.* **2013**, *78*, 3001−3008. (b) Boden, B. N.; Jardine, K. J.; Leung, A. C. W.; MacLachlan, M. J. *Org. Lett.* **2006**, *8*, 1855−1858.

(14) Amato, F.; Phulwale, B. V.; Mazal, C.; Havel, J. *Rapid Commun. Mass Spectrom.* **2015**, *29*, 1125−1134.

(15) (a) Bohlmann, F.; Herbst, P.; Dohrmann, I. *Chem. Ber.* **1963**, *96*, 226−236. (b) Schulte, K. E.; Reisch, J.; Hörner, L. *Chem. Ber.* **1962**, *95*, 1943−1954.

(16) Acheson, R. M.; Lee, G. C. M. *J. Chem. Soc., Perkin Trans. 1* **1987**, 2321−2332.

(17) (a) Ito, H.; Mitamura, Y.; Segawa, Y.; Itami, K. *Angew. Chem., Int. Ed.* **2015**, *54*, 159−163. (b) Goetz, G.; Zhu, X.; Mishra, A.; Segura, J.-L.; Mena-Osteritz, E.; Baeuerle, P. *Chem. - Eur. J.* **2015**, *21*, 7193−7210. (c) Maeda, C.; Masuda, M.; Yoshioka, N. *Org. Lett.* **2013**, *15*, 3566−3569. (d) Masuda, M.; Maeda, C. *Chem. - Eur. J.* **2013**, *19*, 2971−2975. (e) Tokuji, S.; Yorimitsu, H.; Osuka, A. *Angew. Chem., Int. Ed.* **2012**, *51*, 12357−12361. (f) O'Connor, M. J.; Haley, M. M. *Org. Lett.* **2008**, *10*, 3973−3976. (g) Sakai, T.; Satou, T.; Kaikawa, T.; Takimiya, K.; Otsubo, T.; Aso, Y. *J. Am. Chem. Soc.* **2005**, *127*, 8082−8089. (h) Kaikawa, T.; Takimiya, K.; Aso, Y.; Otsubo, T. *Org. Lett.* **2000**, *2*, 4197−4199.

(18) Singh, K.; Virk, T.; Zhang, J.; Xu, W.; Zhu, D. *Chem. Commun.* **2012**, *48*, 12174−12176.

(19) Sprutta, N.; Swiderska, M.; Latos-Grazynski, L. *J. Am. Chem. Soc.* **2005**, *127*, 13108−13109.

(20) Klyatskaya, S.; Dingenouts, N.; Rosenauer, C.; Muller, B.; Höger, S. *J. Am. Chem. Soc.* **2006**, *128*, 3150−3151.

(21) (a) Nilsson, E. J. K.; Johnson, M. S.; Nielsen, C. J. *J. Phys. Chem. A* **2009**, *113*, 1731−1739. (b) Harman, D. G.; Blanksby, S. J. *Org. Biomol. Chem.* **2007**, *5*, 3495−3503.

(22) Martin, R. B. *Chem. Rev.* **1996**, *96*, 3043−3064.

(23) (a) Naik, M. A.; Venkatramaiah, N.; Kanimozhi, C.; Patil, S. *J. Phys. Chem. C* **2012**, *116*, 26128−26137. (b) Yu, Q.-Y.; Liao, J.-Y.; Zhou, S.-M.; Shen, Y.; Liu, J.-M.; Kuang, D.-B.; Su, C.-Y. *J. Phys. Chem. C* **2011**, *115*, 22002−22008. (c) Schmidt-Mende, L.; Kroeze, J. E.; Durrant, J. R.; Nazeeruddin, Md. K.; Grätzel, M. *Nano Lett.* **2005**, *5*, 1315−1320.

(24) Zöphel, L.; Enkelmann, V.; Müllen, K. *Org. Lett.* **2013**, *15*, 804−807.

(25) Thomas, F. G.; Henze, G. In *Introduction to Voltammetric Analysis: Theory and Practice*; CSIRO Publishing, Collingwood, Australia, 2001; p 60.

(26) Bhatt, M. *Tetrahedron* **1964**, *20*, 803−821.

(27) Han, Q.; Li, Q.-J.; He, J.; Hu, B.; Tan, H.; Abliz, Z.; Wang, C.-H.; Yu, Y.; Yang, H.-B. *J. Org. Chem.* **2011**, *76*, 9660−9669.

DOI: 10.1021/acs.joc.6b00814
J. Org. Chem. 2016, 81, 6244−6252